

The structure of the metallic high-pressure Fe_3O_4 polymorph: experimental and theoretical study

This article has been downloaded from IOPscience. Please scroll down to see the full text article.

2003 J. Phys.: Condens. Matter 15 7697

(<http://iopscience.iop.org/0953-8984/15/45/009>)

View [the table of contents for this issue](#), or go to the [journal homepage](#) for more

Download details:

IP Address: 171.66.16.125

The article was downloaded on 19/05/2010 at 17:43

Please note that [terms and conditions apply](#).

The structure of the metallic high-pressure Fe₃O₄ polymorph: experimental and theoretical study

L S Dubrovinsky¹, N A Dubrovinskaia¹, C McCammon¹,
G Kh Rozenberg², R Ahuja³, J M Osorio-Guillen³, V Dmitriev⁴,
H-P Weber⁴, T Le Bihan⁵ and B Johansson³

¹ Bayerisches Geoinstitut, Universität Bayreuth, D-95440 Bayreuth, Germany

² School of Physics and Astronomy, Tel Aviv University, Ramat Aviv, 69978 Tel Aviv, Israel

³ Department of Physics, Uppsala University, S-751 21 Uppsala, Sweden

⁴ SNBL, European Synchrotron Radiation Facility, BP220, F-38043, Grenoble Cedex, France

⁵ European Synchrotron Radiation Facility, BP220, F-38043, Grenoble Cedex, France

Received 7 May 2003

Published 31 October 2003

Online at stacks.iop.org/JPhysCM/15/7697

Abstract

Using electrically- and laser-heated diamond anvil cells at pressures above 40 GPa we synthesized the pure high-pressure Fe₃O₄ phase (h-Fe₃O₄) and performed an *in situ* structural refinement. In good agreement with our *ab initio* calculations we found that h-Fe₃O₄ adopts the CaTi₂O₄-type structure (space group *Bbmm*). Electrical resistivity measurements show that h-Fe₃O₄ is metallic up to at least 70 GPa.

(Some figures in this article are in colour only in the electronic version)

1. Introduction

The structure, properties and high-pressure behaviour of iron oxides have been extensively investigated because of their wide variety of electrical, magnetic, and elastic properties and importance in earth sciences and technology [1, 2]. Magnetite (Fe₃O₄) has an inverse spinel structure at ambient conditions with two different crystallographic iron sites. High-pressure studies of Fe₃O₄ have received special attention due to the geophysical interest and the unclear role of Fe³⁺ in the dynamics and nature of the earth's lower mantle [2, 3].

Studies of the high-pressure polymorph of Fe₃O₄ have given controversial results [3–11]. Mao *et al* [4] demonstrated that magnetite transforms to a high-pressure phase at about 25 GPa. This phase transition was confirmed by Huang and Bassett [5], who determined its temperature dependence. Electrical resistivity measurements [10] revealed compression-induced changes in transport properties of the high-pressure phase, although the conduction mechanism in Fe₃O₄ has not been resolved so far [1, 2, 10]. Based on a limited number of diffraction lines, Mao *et al* [4] proposed a monoclinic symmetry for the high-pressure phase and tentatively assigned all Fe atoms to sixfold coordinated sites. On the other hand, Pasternak

et al [6], based on Mössbauer spectroscopy data, suggested that tetrahedral and octahedral sites characteristic of the inverse spinel structure, albeit distorted, remain the building blocks of the high-pressure phase. Recent x-ray powder diffraction experiments [3, 11] revealed the orthorhombic symmetry of the high-pressure Fe_3O_4 polymorph (h- Fe_3O_4). Fei *et al* [3] proposed the CaMn_2O_4 -type structure (space group $Pbcm$) with highly distorted octahedral (occupied by Fe^{3+}) and eightfold coordinated (bicapped trigonal prism, occupied by Fe^{2+}) sites. The reason for the distortion of the Fe–O polyhedrons in the high-pressure Fe_3O_4 modification is not clear, however, because no Jahn–Teller deformation is expected for the Fe^{3+} and Fe^{2+} cations. In addition, the structure described by Fei *et al* [3] is also not in accordance with Mössbauer data [6]. Haavik *et al* [11] proposed a more symmetric, CaTi_2O_4 -type structure (space group $Bbmm$) for h- Fe_3O_4 . However, the quality of the diffraction data [11] did not allow a structural refinement of h- Fe_3O_4 . Structural information is crucial for the interpretation of the magnetic and electrical properties of the high-pressure modifications of Fe_3O_4 . Here we present results of complex theoretical and experimental (x-ray powder diffraction and electrical resistivity measurements) studies of the orthorhombic high-pressure magnetite polymorph.

2. Theoretical calculations

In order to study the electronic structure and total energy of Fe_3O_4 we have used the full-potential linear muffin-tin-orbital (FPLMTO) method [12, 13]. The calculations were based on the local-density approximation (LDA) and generalized gradient approximation (GGA) and we used the Hedin–Lundqvist [13] and Perdew Burke and Ernzerhof (PBE) [14] parametrization for the exchange and correlation potential. Basis functions, electron densities, and potentials were calculated without any geometrical approximation [12]. These quantities were expanded in combinations of spherical harmonic functions (with a cut-off $l = 8$) inside non-overlapping spheres surrounding the atomic sites (muffin-tin spheres) and in a Fourier series in the interstitial region. The muffin-tin sphere occupied approximately 55% of the unit cell. The radial basis functions within the muffin-tin spheres are linear combinations of radial wavefunctions and their energy derivatives, computed at energies appropriate to their site, principal as well as orbital atomic quantum numbers, whereas outside the muffin-tin spheres the basis functions are combinations of Neuman or Hankel functions [15, 16]. In the calculations reported here, we made use of pseudo-core 3p and valence band 4s, 4p and 3d basis functions for Fe, and valence band 2s, 2p and 3d basis functions for O, with two corresponding sets of energy parameters, one appropriate for the semi-core 3p states, and the other appropriate for the valence states. The resulting basis formed a single, fully hybridizing basis set. This approach has previously proven to give a well converged basis [12]. For sampling the irreducible wedge of the Brillouin-zone we used the special k -point method [17, 18]. In order to speed up the convergence we have associated each calculated eigenvalue with a Gaussian broadening of width 20 mRyd.

As starting models we used the CaMn_2O_4 -type [3] and CaTi_2O_4 -type [11] structures. At fixed volumes of unit cell volumes 278, 223, and 206 Å³ (which corresponds to ambient pressure, 63, and 100 GPa respectively, see below), relaxing the lattice parameters with fixed coordinates of atoms revealed that the CaTi_2O_4 structure gains correspondingly 0.08, 0.41, and 0.49 eV with respect to the CaMn_2O_4 -type structure (figure 1). If the restrictions on the internal parameters are removed at each fixed molar volume at pressures up to 100 GPa, both starting structural models after relaxing give identical results: the fully optimized structure has $Bbmm$ symmetry and belongs to the CaTi_2O_4 structural type (table 1). Theoretical calculations predict that h- Fe_3O_4 orthorhombic phase is a metallic conductor and is magnetic (figure 2).

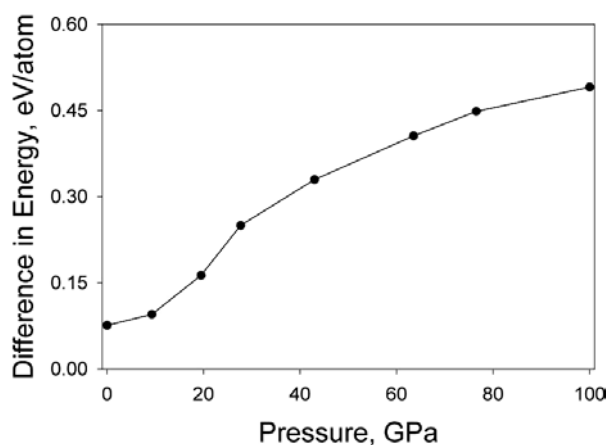


Figure 1. The pressure dependence of the difference in calculated total energies between CaMn₂O₄ (space group *Pbcm*) and CaTi₂O₄ (space group *Bbmm*) structured Fe₃O₄.

Table 1. The structure of orthorhombic h-Fe₃O₄ (space group *Bbmm*) at 41 GPa ($a = 9.326(1) \text{ \AA}$, $b = 9.288(1) \text{ \AA}$, $c = 2.7555(5) \text{ \AA}$).

	Experiment			Theory		
Fe1	0.386 (1)	0.25	0	0.373	0.25	0
Fe2	0.135 (1)	0.076 (3)	0	0.128	0.071	0
O1	0.048 (2)	0.25	0	0.028	0.25	0
O2	0.210 (1)	0.616 (1)	0	0.221	0.620	0
O3	0.5	0	0	0.5	0	0

3. Experimental method

To check the theoretical predictions we conducted several series of high-pressure experiments. The pure and ⁵⁷Fe enriched samples of magnetite were synthesized as already described [6, 11]. The lattice parameters of the starting materials varied between 8.3963(5) and 8.3969(5) Å, in good agreement with Fleet [19]. The details of the experiments performed with electrically- and laser-heated DAC are described by Dubrovinsky *et al* [20–22]. At ESRF powder diffraction experiments were conducted at beam lines BM01 and ID30. At the BM01 beam line the data were collected with the MAR345 detector using an x-ray beam with 0.6996 Å wavelength and 50 μm × 50 μm cross section, and at ID30 we used a MAR345 or Bruker CCD area detector and a highly focused beam of 10 μm × 15 μm with 0.3738 Å wavelength. The detector-to-sample distance varied in different experiments from 170 to 350 mm. Diamonds were mounted on seats made of B₄C or BN, allowing us to collect the complete Debye rings to 0.95 Å. The collected images were integrated using the Fit2D program in order to obtain a conventional diffraction spectrum. The Rietveld refinements of powder x-ray diffraction data were carried out using the GSAS program [23]. As internal pressure standards we used NaCl, Pt or Au powder mixed with the sample in the mass proportion approximately 1:1 for NaCl and 1:20 for metals. All loadings of the DAC were made in an inert atmosphere (Ar or He).

Four-probe DC resistance measurements were carried out with 3–6 μm thick Pt electrodes as a function of pressure and temperature using a technique similar to that described by Rozenberg *et al* [9]. The gaskets were coated with isolating corundum-based cement. No pressure medium was used in the electrical resistivity experiments.

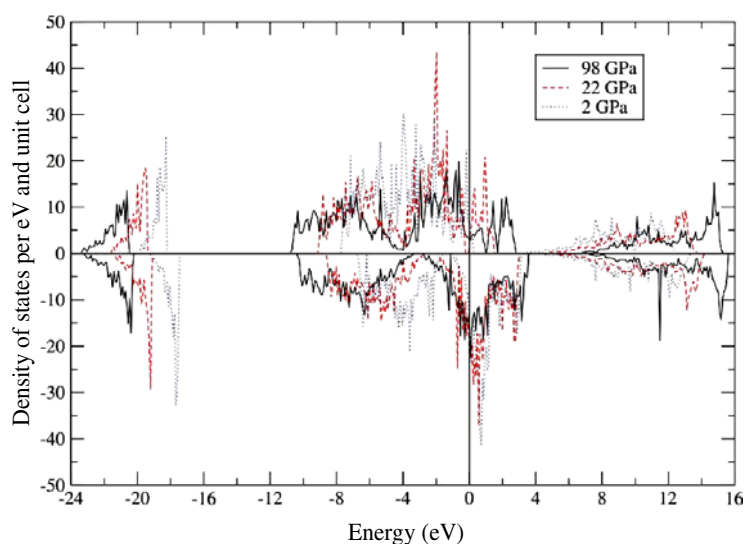


Figure 2. The calculated total density of states (DOS) for h-Fe₃O₄ with CaTi₂O₄-type structure (space group *Bbmm*) at different pressures. The Fermi level is set at zero energy and is marked by a vertical line. The high-pressure CaTi₂O₄-type phase is magnetic because spin-up and spin-down bands are different and there is therefore a net spin polarization.

4. Results and discussion

Figure 3 shows examples of experimental diffraction patterns collected on Fe₃O₄. At pressures above 19 GPa we observed the appearance of new reflections, in good agreement with literature data [4–6]. With increasing pressure at ambient temperature the amount of the high-pressure phase increased (figure 3), but the reflections of the low-pressure cubic phase could be easily traced to at least 60 GPa. The sluggish nature of the phase transformation between the Fe₃O₄ polymorphs at room temperature was also observed earlier [3–6, 11]. For example, Pasternak *et al* [6] estimated that only about 60% of magnetite transforms into a high-pressure modification on compression to 66 GPa at ambient temperature. However, heating greatly facilitates the phase transformation [3, 5]. Heating at 41 GPa and temperatures between 1000 K and 1200 K for 1 h in the laser-heated DAC allowed us to synthesize nearly pure h-Fe₃O₄ phase (figure 3). The diffraction pattern of h-Fe₃O₄ could be easily indexed in an orthorhombic cell [3, 11] (figures 3, 4).

The unit cell parameters of the h-Fe₃O₄ phase were determined on decompression in the pressure range 45–9 GPa (12 data points) (figure 5). After each pressure decrease the stress in the sample was relaxed by external electrical heating of the cell at 600–650 K for 1–1.5 h. The molar volume (*V*) versus pressure (*P*) data were fitted to a third-order Birch–Murnaghan equation of state [24] (EOS):

$$P = 1.5K_{300}[(V_0/V)^{7/3} - (V_0/V)^{5/3}][1 - 0.75(4 - K')\{(V_0/V)^{2/3} - 1\}] \quad (1)$$

(*K*₃₀₀, *K'*, and *V*₀ are the bulk modulus, its pressure derivative, and the molar volume at zero pressure and 300 K, respectively).

The fit gave values for *K*₃₀₀ and *V*₀ of 198(5) GPa and 41.84(7) cm³ mol⁻¹, respectively (*K'* = 4 was fixed) (figure 5), slightly lower than the values reported by Haavik *et al* [11] but in good agreement with the results of *ab initio* calculations (184 GPa).

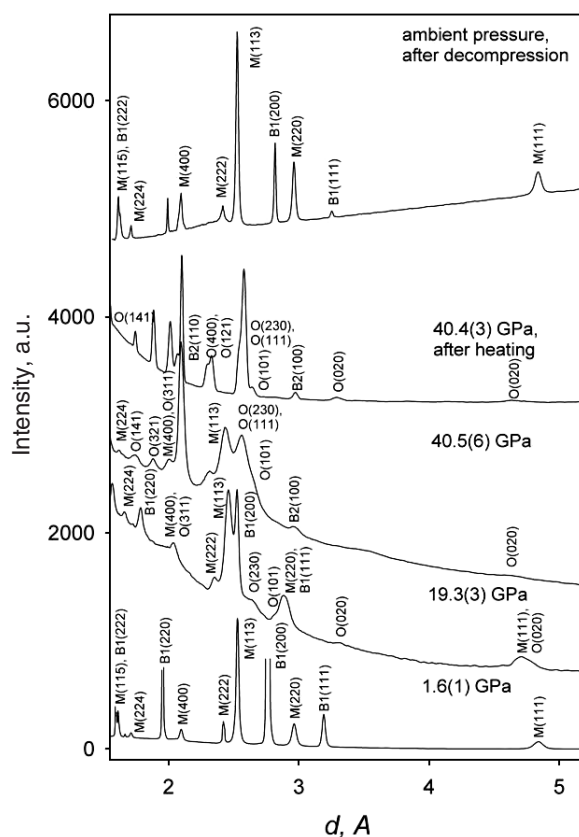


Figure 3. Examples of x-ray diffraction patterns obtained in experiments with Fe₃O₄ (B1 for NaCl (B1, *Fm*3*m* space group), B2 for NaCl (B2, *Pm*3*m* space group), M for cubic magnetite, O for orthorhombic h-Fe₃O₄).

After complete decompression of the samples treated at high temperature and pressures up to 60 GPa, we observed only initial cubic magnetite with the same lattice parameters as the starting material (figure 3). This implies that Fe₃O₄ is stable as a compound at least up to 60 GPa and 1200 K.

For structural refinement the sample was synthesized in an electrically heated DAC by treatment of the initially cubic magnetite at 40(1) GPa and 950(25) K for 6 h. NaCl was used as a pressure transmitting medium and internal pressure standard. Figure 4 and table 1 shows the results of the refinements. ‘Visual’ inspection of the quality of the fit obtained for CaMn₂O₄- and CaTi₂O₄-structural types (figures 4(a), (b)) shows that they are quite similar. Using fixed atomic coordinates as reported by Fei *et al* [3] (optimised lattice parameters, background and line profiles) for the CaMn₂O₄-type structure we obtained $wRp = 5.2$, $Rp = 3.2$, $\chi^2 = 0.33$ (in all the calculations described here atomic thermal factors were fixed at the values 0.025 for all atoms). For the CaTi₂O₄-structural type starting from the atomic coordinates proposed by Haavik *et al* [11] (optimised lattice parameters, atomic coordinates, background and line profiles) we obtained $wRp = 3.4$, $Rp = 2.1$, $\chi^2 = 0.14$. This could indicate that the CaTi₂O₄ structure gives a better description of the experimental observations than the CaMn₂O₄ model. Comparison of Durbin–Watson statistic parameters (1.94 for CaTi₂O₄

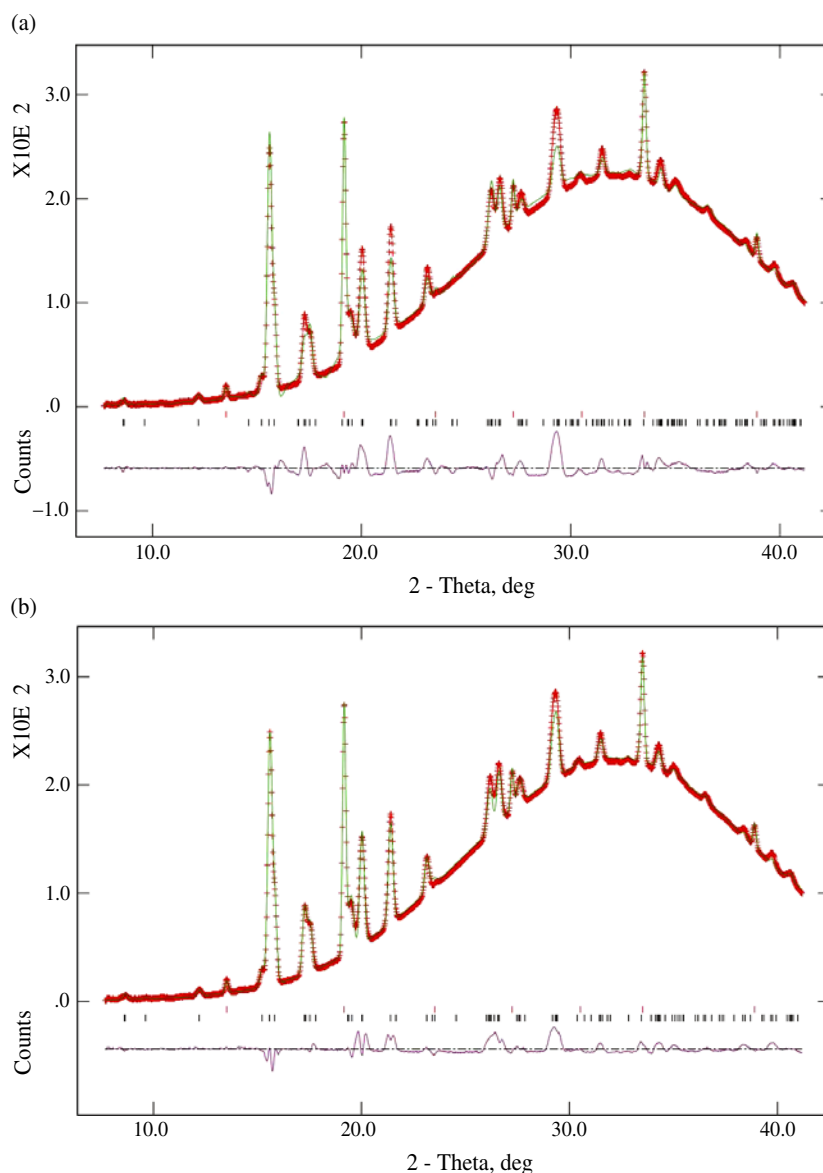


Figure 4. An example of profile-fitted x-ray diffraction data obtained at 41 (1) GPa from a mixture of orthorhombic Fe_3O_4 (bottom ticks) and NaCl (upper ticks). (a) CaMn_2O_4 -type structure (space group $Pbcm$, atomic coordinates fixed on the values reported by Fei *et al* [3]). (b) CaTi_2O_4 -type structure (space group $Bbmm$, optimised atomic coordinates given in table 1). The GSAS program package [23] was used in the Rietveld refinement.

structural type and 1.82 for CaMn_2O_4 structural type) confirms this conclusion. However, even more important is that if we freely optimise the atomic parameters (optimisation of lattice parameters, atomic coordinates, background and line profiles) starting from the atomic parameters [3] of CaMn_2O_4 (space group $Pbcm$), the resulting structure is identical to that obtained for CaTi_2O_4 (space group $Bbmm$) (table 1). It should be noted that the theoretically

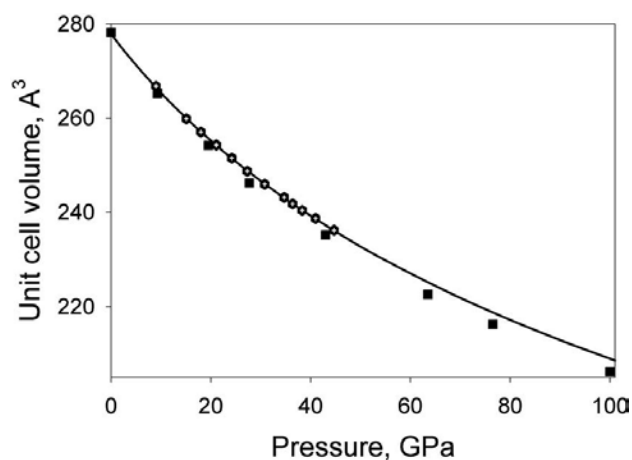


Figure 5. The pressure dependence of the volume of the phases of the orthorhombic high-pressure modification Fe₃O₄. Experimental data are shown by hexagons (uncertainties in pressure and volume are within the symbols), and the results of *ab initio* calculations are shown by squares. The full curve represents the Birch–Murnaghan equation of state fitted for the experimental data, plotted with parameters $K_{300} = 198$ (5) GPa, $K' = 4$ (fixed), $V_0 = 277.9$ (4) Å³/unit cell.

calculated structural parameters are close to the experimental ones (table 1) and are in good agreement with structural data by Haavik *et al* [11].

In the refined structure the Fe atoms occupy octahedra (Fe2–O distances (in Å) are 1.808(1), 1.919(1), 1.995(2) (×2), 2.024(2) (×2)) and trigonal prisms (Fe1–O distances (in Å) are 2.045(1) (×2), 2.065(2) (×2)) (figure 6). The next two neighbouring oxygen atoms around the Fe1 position are found at a distance 2.554(3) Å and, if considered together with six other O atoms, form a ‘bicapped prism’ (with both triangular faces capped). A similar bicapped prism is known for eightfold coordinated Ca in the CaTi₂O₄ structure [25]. However, due to the much smaller size of the Fe²⁺ ions in comparison to Ca²⁺ in h-Fe₃O₄, the effective coordination of the Fe2 site decreases from 8 to 6.

The average Fe1–O distance is 2.058 Å, while Fe2–O is 1.961 Å, suggesting that Fe²⁺ occupies trigonal prisms, while Fe³⁺ sits in an octahedron. At 41 GPa the differences in the Fe–O distances from the Fe1 position are about 1%, and in the Fe2 position about 12%. For comparison, in h-Mn₃O₄ (CaMn₂O₄ structural type [25]) at 39 GPa Mn³⁺–O varies by 26% and Mn²⁺–O varies by 19%. Such significant distortion of the Mn–O polyhedron is the consequence of the Jahn–Teller effect. For Fe³⁺ and Fe²⁺ no Jahn–Teller deformation is expected and as a result the FeO₆ octahedra and prisms in h-Fe₃O₄ are much more regular.

The shortest Fe–Fe distance in orthorhombic Fe₃O₄ at 41 GPa is ~2.75 Å between atoms in the trigonal prisms that share common faces. This distance can be compared with the shortest Fe–Fe distance in the high-pressure modification of Fe₂O₃ at 60 GPa (~2.71 Å) [26] or in the high-pressure phase of FeO [27–29] (2.70–2.75 Å at 65–75 GPa). Both these compounds are thought to be metallic conductors at corresponding conditions [30, 31]. Our *ab initio* calculations (see above) suggest that h-Fe₃O₄ is also metallic, in contrast to Morris and Williams [10], who reported semiconducting behaviour of Fe₃O₄ on compression to 48 GPa at temperatures between 258 and 300 K. However, we know now that compression to 48 GPa at ambient temperature is not sufficient for complete structural phase transformation from the cubic to orthorhombic phases. Morris and Williams [10] laser-heated the sample at 48 GPa. However, it is not possible to transform completely a 25 μm thick sample with one-side

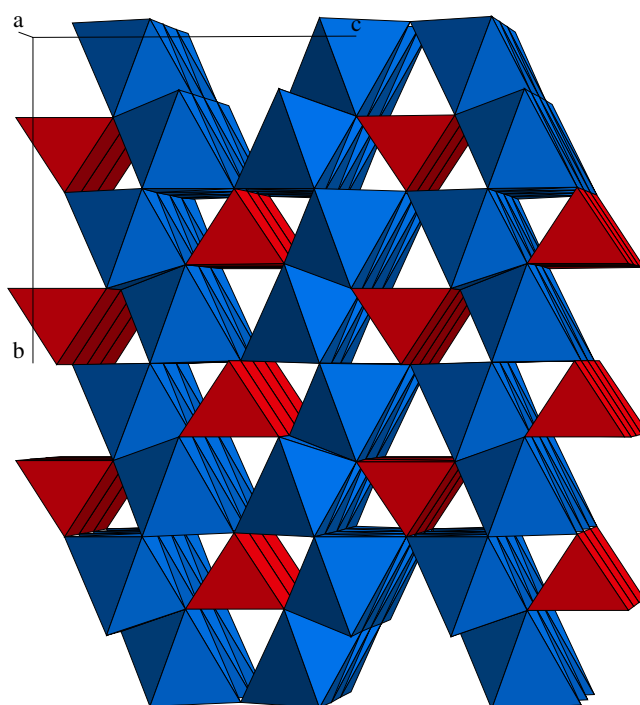


Figure 6. Polyhedral model for the orthorhombic (space group *Bbmm*) Fe₃O₄ phase (Fe1 prisms and Fe2 octahedra).

laser-heating in a Mao–Bell-type cell. Moreover, Morris and Williams [10] used MgO as a pressure medium and it could cause a chemical reaction between magnetite and MgO at high temperature. Indeed, we found that when the initial cubic magnetite is compressed to 51 GPa, it behaves as a semiconductor at temperatures between 90 and 420 K (figure 7). However, after electrical heating at temperatures between 1000 K and 1100 K for 5 h we observed that the reflectivity of the sample increased and the resistance decreased significantly, and the slope of the $R(T)$ curve changed to positive (figure 7). This implies that fully transformed h-Fe₃O₄ is metallic. Moreover, when treated at high-temperature at 51 GPa the sample continued to be metallic on decompression to 24 GPa (figure 7).

5. Summary

Our combined theoretical and experimental studies revealed the complex nature of the high-pressure polymorph of magnetite, the oldest known magnetic material. We demonstrated that the long-standing inconsistency between structural and electrical resistivity data at high pressure is mostly due to sluggish kinetics of the phase transition between the cubic and orthorhombic phases at ambient temperatures, and difficulties with the synthesis of the high-pressure polymorph. The first structural refinement of the orthorhombic Fe₃O₄ structure from x-ray powder diffraction data collected at 40 GPa from sample synthesized at 950 K shows that h-Fe₃O₄ adopts the CaTi₂O₄-type structure (space group *Bbmm*). We found that h-Fe₃O₄ is metallic.

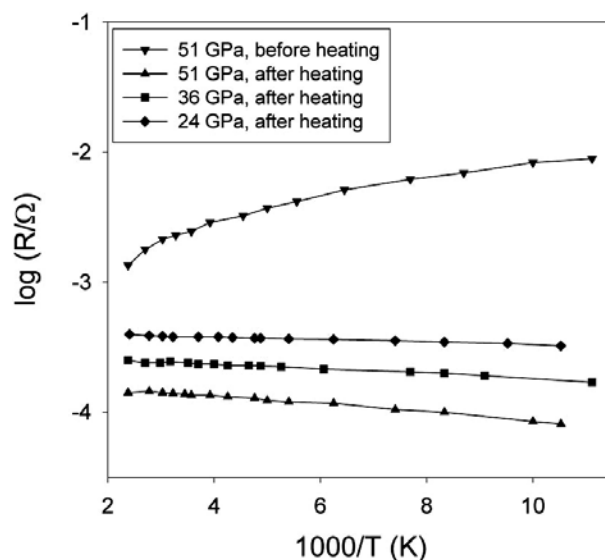


Figure 7. The temperature dependence of $\log_{10}(R)$ at various pressures. The initial cubic magnetite compressed to 51 GPa behaves as a semiconductor at temperatures between 90 K and 420 K (inverse triangles). However, after electrical heating at temperatures between 1000 K and 1100 K for 5 h we observed that the resistivity of the sample decreased significantly and on cooling to 90 K the resistivity decreased further (triangles), implying that fully transformed h-Fe₃O₄ is metallic. Moreover, the sample treated at high temperature and 51 GPa continued to be metallic on decompression to 36 GPa (squares) and 24 GPa (diamonds).

Acknowledgments

The comments of two anonymous reviewers were useful and allowed us to improve our presentation. This work was supported by a DFG grant.

References

- [1] Cox P A 1992 *Transition Metal Oxides* (Oxford: Clarendon) p 284
- [2] Hemley R J (ed) 1998 *Ultrahigh-Pressure Mineralogy: Physics and Chemistry of the Earth's Deep Interior* (*Rev. Mineralogy* vol 37) (Washington, DC: Mineralogical Society of America) p 671
- [3] Fei Y, Frost D J, Mao H K, Prewitt C T and Häusermann D 1999 *Am. Mineral.* **84** 203–6
- [4] Mao H K, Takahashi T, Basset W A, Kinsland G L and Merrill L 1974 *J. Geophys. Res.* **79** 1165–70
- [5] Huang E and Basset W A 1986 *J. Geophys. Res.* **91** 4697–703
- [6] Pasternak M P, Nasu S, Wada K and Endo S 1994 *Phys. Rev. B* **50** 6446–9
- [7] Finger L W, Hazen R M and Hofmeister A M 1986 *Phys. Chem. Minerals* **13** 215–20
- [8] Nakagiri N, Manghni M H, Ming L C and Kimura S 1986 *Phys. Chem. Minerals* **13** 238–44
- [9] Rozenberg G Kh, Hearne G R, Pasternak M P, Metcalf P A and Honig J M 1996 *Phys. Rev. B* **53** 6482–7
- [10] Morris E R and Williams Q 1997 *J. Geophys. Phys.* **102** 18139–48
- [11] Haavik C, Stølen S, Fjellvåg H, Hanfland M and Häusermann D 2000 *Am. Mineral.* **85** 514–23
- [12] Wills J M and Cooper B R 1987 *Phys. Rev. B* **36** 3809–15
- [13] Hedin L and Lundqvist B L 1971 *J. Phys. C: Solid State Phys.* **4** 2064–8
- [14] Perdew J P, Burke K and Ernzerhof M 1996 *Phys. Rev. Lett.* **77** 3865
- [15] Skriver H L 1984 *The LMTO Method* (Berlin: Springer)
- [16] Andersen O K 1975 *Phys. Rev. B* **12** 3060
- [17] Chadi D J and Cohen M L 1973 *Phys. Rev. B* **8** 5747
- [18] Froyen S 1989 *Phys. Rev. B* **39** 3168
- [19] Fleet M E 1981 *Acta Crystallogr. B* **37** 917–20

-
- [20] Dubrovinsky L S *et al* 1997 *Nature* **388** 362–6
 - [21] Dubrovinsky L S *et al* 1999 *High Pressure High Temp.* **31** 553–9
 - [22] Dubrovinsky L S *et al* 2000 *Phys. Rev. Lett.* **84** 1720–3
 - [23] Larson A C and Von Dreele R B 1994 *LAUR 86* Los Alamos National Laboratory
 - [24] Anderson O L 1995 *Equations of State of Solids for Geophysics and Ceramic Science* (Oxford: Oxford University Press) p 405
 - [25] Paris E, Ross C R and Olijnyk H 1992 *Eur. J. Mineral.* **4** 87–93
 - [26] Rozenberg G Kh *et al* 2002 *Phys. Rev. B* **65** 064112
 - [27] Fang Z, Solovyev I V, Sawada H and Terakura K 1999 *Phys. Rev. B* **59** 762–4
 - [28] Fei Y and Mao H K 1994 *Science* **266** 1678–81
 - [29] Dubrovinsky L S *et al* 2000 *Science* **289** 430–2
 - [30] Pasternak M P *et al* 1999 *Phys. Rev. Lett.* **82** 4663–7
 - [31] Knittle E and Jeanloz R 1991 *J. Geophys. Res.* **96** 16169–80